THE JOURNAL OF PHYSICAL CHEMISTRY B

ARTICLE

pubs.acs.org/JPCB

Electrochemistry of Cytochrome c_1, Cytochrome c_{552}, and Cu_A from the Respiratory Chain of *Thermus thermophilus* Immobilized on Gold Nanoparticles

Thomas Meyer,[†] Julien Gross,[†] Christian Blanck,[‡] Marc Schmutz,[‡] Bernd Ludwig,[§] Petra Hellwig,[*,†] and Frederic Melin[*,†]

[†]Laboratoire de Spectroscopie Vibrationnelle et Electrochimie des Biomolécules (Institut de Chimie, UdS), 1 Rue Blaise Pascal 67008 Strasbourg Cedex, France

[‡]Institut Charles Sadron (UPR22-CNRS, UdS), 23 rue du Loess BP 84047 67034 Strasbourg Cedex 2, France

[§]Institute of Biochemistry, Molecular Genetics Biocenter, Max-von-Laue-Str., 9, 60438 Frankfurt, Germany

Supporting Information

ABSTRACT: The electrochemical behavior of three proteins fragments from the respiratory chain of the extremophilic bacterium *Thermus thermophilus*, namely, cytochrome c_1 (Cyt-c_1), cytochrome c_{552} (Cyt-c_{552}), and Cu_A, immobilized on three-dimensional gold nanoparticles electrodes was investigated by cyclic voltammetry. The gold nanoparticles were modified by either dithiobissuccinimidyl propionate (DTSP) or a mixed self-assembled monolayer of 6-mercaptohexan-1-ol and hexanethiol, depending on the surface of the protein. High surface coverages with enzymes and good electron transfer rates were achieved in the case of Cyt-c_1 immobilized on DTSP-modified gold nanoparticles and Cyt-c_{552} or Cu_A immobilized on mixed SAMs−modified gold nanoparticles. Interestingly, high surface coverages with Cu_A were also observed on DTSP-modified gold nanoparticles, but a slower electron transfer rate was determined in this case. The gold nanoparticle/protein assemblies were characterized by surface-enhanced IR spectroscopy and transmission electron microscopy.

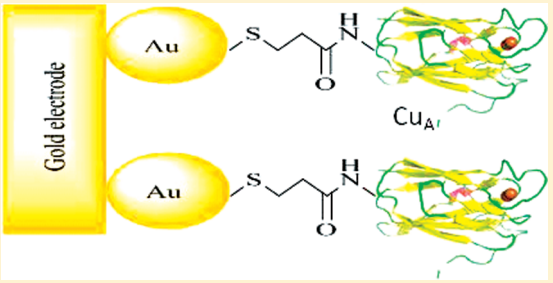

1. INTRODUCTION

Enzyme-based electrodes have attracted attention due to their promising applications in biosensor[1] or biofuel cell[2−5] devices. Since diffusion to the electrode is often the rate-determining step of the enzyme electrochemistry in solution, electrochemical studies of the enzymatic mechanisms also require the immobilization of the protein on the electrode.[6−8] Most efforts have focused on finding an efficient immobilization procedure for the redox enzymes on the surface of the electrodes.[3,4,9] The selected method should at the same time provide a suitable environment for the enzyme, since this will directly affect the lifetime of the biodevice. While not exceeding a few hours in solution, the activity of the enzyme could be extended in recent approaches to a few days and even a few months once immobilized.[10] Another crucial aspect that will affect the efficiency or the sensitivity of the biodevice is the amount of protein immobilized. Finally, it is necessary to achieve an efficient electron transfer (ET) between electrode and enzyme. Unfortunately, redox cofactors are usually buried inside the protein shell, which often prevents direct electron transfer (DET) between the electrode and the enzyme. Therefore, redox mediators are commonly used and are either coimmobilized on the electrode or dissolved in the buffer solution. However, the stability of these mediators and their easy diffusion away from the surface of the electrode can limit the lifetime of the enzyme-based system. New procedures of immobilization that maintain the protein activity and allow a fast electron transfer between the enzyme and the electrode without the use of mediators have been described. Most noticeably, enzymes have been entrapped in membranes such as Nafion,[11] in redox polymers,[2] in carbon pastes, and in sol−gel matrices.[12] Covalent linkage and attachment through affinity interactions to the surface of electrodes are still commonly used methods.[13−15]

One of the most promising procedures of immobilization consists of using metal nanoparticles[16−22] that act as a relay in the long-range electron transfer between the electrode and the cofactors. Most frequently a monolayer of gold nanoparticles has been deposited on the electrode, resulting in an enhanced DET rate with various proteins, such as glucose oxidase,[16] galactose oxidase,[23] laccase,[24] myoglobine,[25] hemoglobin,[25] and cytochrome c[26] attached to these nanoparticles. Very recently, porous three-dimensional gold nanoparticle electrodes were obtained by drop-casting a concentrated gold colloid on the

Received: March 21, 2011
Revised: April 19, 2011
Published: May 10, 2011

surface of a polycrystalline gold substrate.[27] These electrodes allowed both an exceptionally high surface coverage by cytochrome *c* and a reversible DET with the enzyme. In these studies, cytochrome *c* was adsorbed on the surface of the nanoparticles, through an electrostatic interaction between its charged surface lysine residues and carboxylic acid-terminated alkanethiols. The nature of the ligand of the gold nanoparticles was found to be crucial, since it dramatically influences the conformation of the adsorbed protein and consequently its redox activity.[28,29]

Here we report the immobilization of three water-soluble protein fragments from the respiratory chain of *Thermus thermophilus,* which differ by their cofactor and the nature of their surface, on 15 nm gold nanoparticles. Cytochrome c_1 is a recently isolated subunit of the respiratory complex III that participates in the electron transfer path. We study here a soluble fragment of this protein containing the cofactor (9.4 kDa).[30] The midpoint potential of this key protein from *T. thermophilus* has not yet been reported. Cytochrome c_{552} (14.2 kDa),[31] the second studied protein, mediates the electron transfer between the cytochrome c_1 in complex III and the respiratory complex IV (cytochrome *c* oxidase). Interestingly, this protein does not have any charged residues on its surface in the vicinity of the heme crevice, unlike most of other *c* type cytochromes.[31] The last studied protein is Cu_A, the initial electron acceptor in complex IV. It contains a binuclear copper site in which the metallic atoms are bridged by sulfur atoms from cysteine residues.[32] Here we study a soluble fragment of this protein containing the cofactor (14.9 kDa).[33] In the respiratory chain of *T. thermophilus*, these three proteins are successive redox partners. They have recently attracted attention since their interaction is mainly hydrophobic, the high working temperatures of the bacterium providing a possible explanation.[34−37] The largely uncharged surface of these proteins offers an interesting opportunity to study the immobilization on gold nanoparticles. The new enzyme-modified gold nanoparticles created here have been characterized by transmission electron microscopy (TEM) and surface-enhanced IR absorption spectroscopy (SEIRAS). The electrochemical behavior of the immobilized enzymes has been studied by cyclic voltammetry and directly compared to their behavior in solution.

2. EXPERIMENTAL SECTION

Chemicals. Sodium citrate, hydrogen tetrachloroaurate trihydrate ($HAuCl_4 \cdot 3H_2O$), dithiobissuccinimidyl propionate (DTSP), 6-mercaptohexan-1-ol, hexanethiol, cytochrome *c* from horse heart, potassium dihydrogen phosphate (KH_2PO_4), disodium hydrogen phosphate (Na_2HPO_4), dimethyl sulfoxide (DMSO), and ethyl alcohol (EtOH) were purchased from Sigma-Aldrich and used without further purifications.

Production and Purification of the Proteins. The soluble fragment of the cytochrome c_1 (Cyt-c_1) subunit of the bc_1 complex of *T. thermophilus* was heterologously expressed and purified as described earlier[30] and the soluble cytochrome c_{552} (Cyt-c_{522}) as published.[38] The water-soluble Cu_A protein from *T. thermophilus* was prepared in the laboratory of Dr. James A. Fee by Dr. Ying Chen using the method of Slutter et al.[33] and was a generous gift to this work.

Preparation of the Gold Colloid. Following the procedure proposed initially by Turkevich[39] and refined by Frens,[40] a solution of $HAuCl_4$ (55 mg) was boiled in Milli-Q water (140 mL), and subsequently an aqueous solution of sodium citrate (160 mg in 13 mL of water) was added. The temperature was maintained for 15 min and then the solution was allowed to cool down to room temperature. The concentrated gold colloid was obtained by centrifugation of this stock solution at 10*g* for 30 min and redispersion in 1% of the initial volume. The absorption measurements were recorded at room temperature using a Cary 300 Scan UV−visible spectrometer (Varian).

Electrochemistry. After mechanical polishing with 1 and 0.05 μm alumina powders, a 2 mm diameter polycrystalline gold disk electrode was activated in 0.1 M H_2SO_4 by maintaining the potential at 2.0 V for 5 s and then −0.35 V for 10 s and then cycling 100 times between −0.35 and 1.5 V at 4 V/s. A final scan was done at 0.1 V s^{-1} between −0.35 and 1.5 V, and the effective area of the electrode was estimated by integration of the Au−O reduction peak at 1.1 V and assuming a value of 390 μC cm^{-2} for a gold oxide surface.[41] Immediately after drying, one drop of the concentrated gold colloid was deposited on the surface of the electrode and allowed to evaporate. Two further deposits of gold nanoparticles were made. The electrode was then plunged in 0.1 M H_2SO_4 and the potential cycled between −0.35 and 1.5 V until stabilization of the signal, and the new gold area was estimated by integration of the Au−O reduction peak. The electrode was then left overnight in either a 2 mM solution of dithiobissuccinimidyl propionate in DMSO or in a 1 mM solution of hexanethiol and 6-mercaptohexan-1-ol in EtOH. After rinsing with fresh solvent and drying, 2 μL of a 0.2 mM solution of the protein in 50 mM KPi buffer (pH 8) was deposited on the electrode and left for 5 h at 4 °C. The electrode was finally rinsed several times with a fresh buffer solution to remove the excess of proteins. The voltammograms were obtained using a conventional three-electrode setup connected to a Princeton Applied Research VERSASTAT 4 potentiostat. A Platinum wire was used as the counter electrode and an aqueous 3 M AgCl/Ag electrode as reference electrode [add 0.208 V for a standard hydrogen electrode (SHE)]. All the potentials mentioned in the text are referenced to the SHE electrode. All buffer solutions were flushed with argon for at least 10 min before the measurements.

SEIRAS Studies. A 20 nm thick gold substrate was sputtered on the surface of the silicon internal reflection element from an ATR cell unit (current 30 A, argon pressure 0.06 mbar, deposition time 10 min). Two microliters of a concentrated gold colloid was deposited on this substrate and allowed to dry. Then 2 μL of either a 2 mM solution of dithiobissuccinimidyl propionate in DMSO or a 1 mM solution of hexanethiol and 6-mercaptohexan-1-ol in EtOH was deposited on the surface. After 30 min, the solution was removed and the surface was rinsed with fresh solvent. Finally, 2 μL of a 0.1 mM protein solution in KPi buffer (pH 8) was deposited. After 1 h, the surface was rinsed several times with a fresh buffer solution. SEIRAS spectra were obtained for each modification step using a Bruker Vertex 70 spectrometer fitted with a Harrick ATR cell, and 256 spectra with 4 cm^{-1} resolution were averaged. The respective solvents or buffers were taken as reference for the spectra.

TEM Studies. The procedure to prepare the gold nanoparticles/Cyt c_1 assemblies was slightly adapted to meet the requirements for the TEM grid preparation, as well as protein observation. The Cyt-c_1 was added to the nanoparticles in solution. The DTSP modifier was first added to 0.05 mM solution of Cyt-c_1 in 50 mM KPi buffer (pH 8) and the mixture vigorously stirred for 3 h at 4 °C. Then 1 μL of the concentrated gold colloid was added. No aggregation of the nanoparticles was observed in this case. The mixture was again stirred for 3 h and centrifuged for 10 min at 10*g* to remove the excess of protein. The supernatant was

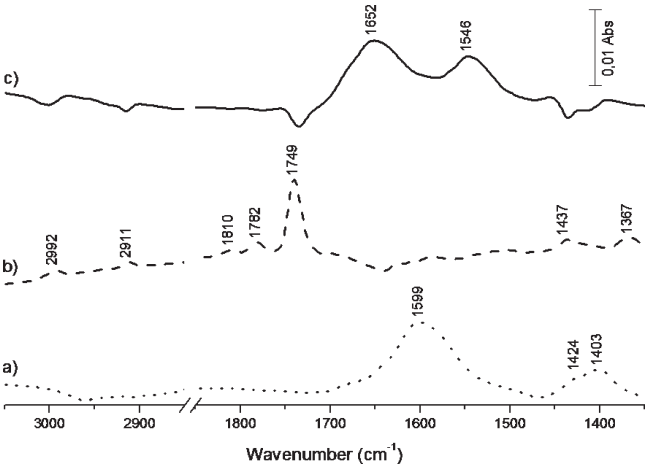

Figure 1. SEIRAS difference spectra obtained on a 20 nm thick gold substrate after deposition of gold nanoparticles (spectrum a), subsequent addition of DTSP (spectrum b), and then immobilization of Cyt-c_1 (spectrum c).

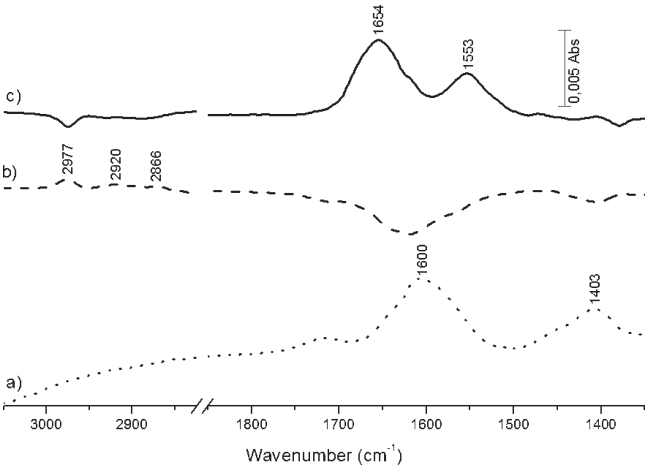

Figure 2. SEIRAS difference spectra obtained on a 20 nm thick gold substrate after deposition of gold nanoparticles (spectrum a), subsequent addition of a (1/1) mixture of 6-mercaptohexan-1-ol and hexanethiol (spectrum b), and then immobilization of cyt-c_{552} (spectra c).

discarded, and the precipitated gold nanoparticles were redispersed in 50 mM KPi buffer (pH 8). The centrifugation was repeated once. Five microliters of the solution was deposited onto a freshly glow discharged carbon-covered copper grid (400 mesh). The solution was left for 1 min, and then the grid was negatively stained with 5 μL of uranyl acetate (1% in water) for another 1 min and finally air-dried. The grids were observed at 200 kV with a Tecnai G2 (FEI) microscope. Images were acquired with an Eagle 2k (FEI) ssCCD camera.

3. RESULTS AND DISCUSSION

Modification of the Gold Working Electrodes. Three-dimensional gold nanoparticle electrodes were obtained following the procedure of Nakamura et al.[27] The gold nanoparticles were synthetized by reduction with sodium citrate of a gold(III) chloride solution, and their average diameter (15 nm) was determined from the plasmon band intensity in the UV/visible spectrum[42] (see Supporting Information S2). Three drops of a concentrated solution of these nanoparticles were deposited on a gold disk working electrode, bringing the specific surface area of gold from ca. 0.1 to 8 cm^2, as estimated from integration of the Au−O reduction peak at 1.1 V (see Supporting Information S3). The observation of two oxidation peaks at 1.4 and 1.6 V vs SHE was taken as a proof of the presence of the gold nanoparticles on the electrode.[27] The different nature of the surface of Cyt-c_{552} and the soluble fragment of Cyt-c_1 from *T. thermophilus* led us to try different kind of thiols. In the case of cytochrome c_1, the electrode was further modified with dithiobissuccinimidyl propionate (DTSP), which is, by removal of the succinimidyl group, able to form at pH 8 a covalent bond with a surface NH_2 group of the enzyme.[43,44] For comparison, we have also tested this immobilization procedure with the model protein, cytochrome *c* from horse heart. In the case of cytochrome c_{552}, the electrode was modified with a mixed SAM of 6-mercaptohexan-1-ol and hexanethiol (1/1 ratio). These SAMs were previously shown to be a well-adapted support for the immobilization of Cyt-c_{552} and to mimic the interaction surface of its natural redox partner, the Cu_A domain of ba_3 oxidase.[45−47] Mixed SAMs are also convenient for Cu_A immobilization,[48] but quite unexpectedly we have found that DTSP works also for this protein, albeit less efficiently. The enzymes were subsequently immobilized by deposition of 2 μL of a 0.1 mM protein solution in KPi 50 mM (pH 8) buffer on the modified electrodes and incubation for 5 h at 4 °C.

Characterization of the Protein-Modified Gold Nanoparticles. The immobilization procedure was followed by SEIRAS on a 20 nm thick gold substrate sputtered on the surface of a silicon internal reflection crystal (Figure 1). This technique was selected because it exclusively shows signals from adsorbed molecules.[49,50] After deposition of the gold nanoparticles, the SEIRAS spectrum shows the large bands characteristic for citrates (bands of carboxylate groups at 1599 and 1400 cm^{-1}),[51] which are stabilizing the particles. These bands are replaced by those of the succinimidyl ester after respective modification of the gold nanoparticles. In particular, the CO stretching bands at 1740, 1782, and 1810 cm^{-1},[49] as well as the C−H stretching bands at 2992 and 2911 cm^{-1}, are evident. Further immobilization of cytochrome c_1 yields the characteristic amide I band between 1700 and 1600 cm^{-1} and amide II band between 1600 and 1500 cm^{-1}. These signals include the coordinates of the polypeptide backbone.[52,53] The maximum of the amide I band found here (1652 cm^{-1}) suggests that α-helical secondary structure elements are predominant in this protein.[52] The additional negative bands at 1740 and 1437 cm^{-1} confirm the removal of the succinimide moiety. Stable spectra are obtained within 1 h, and even after extensive cleaning of the surface, the protein bands are persistent, which proves their successful immobilization.

The mixed SAM of 6-mercaptohexan-1-ol and hexanethiol gives C−H stretching signals at 2977, 2920, and 2860 cm^{-1} (Figure 2b). Subsequent immobilization of Cyt-c_{552} (Figure 2c) yields an amide I band centered at 1654 cm^{-1} typical of α-helical secondary elements, whereas immobilization of Cu_A (see Supporting Information S4) yields an amide I band at 1635 cm^{-1}, typical of predominant β-sheet elements.[52] This is in line with the known structures,[31,32] confirming the integrity of the proteins after immobilization.

The gold nanoparticle/cyt c_1 assemblies were also analyzed by transmission electron microscopy. All the observed nanoparticles (Figure 3b) exhibited some proteins grafted on their surface, which are seen as a white rim around the gold surface due to the

dx.doi.org/10.1021/jp202656w |J. Phys. Chem. B 2011, 115, 7165–7170

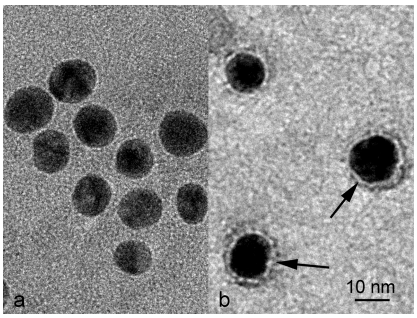

Figure 3. TEM images of negatively stained gold nanoparticles before (a) and after (b) immobilization of soluble Cyt-c_1.

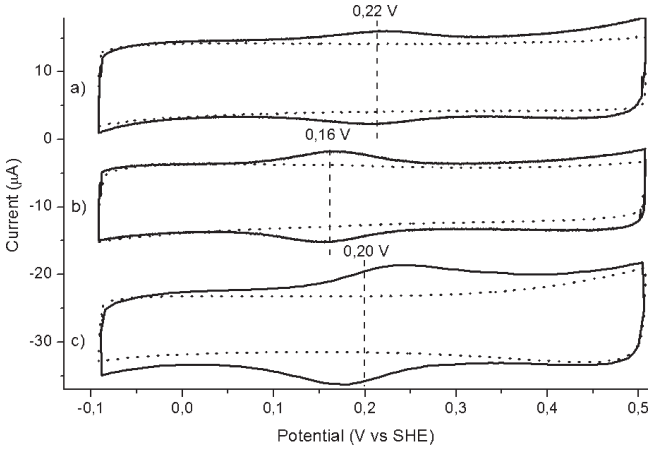

Figure 4. Cyclic voltammetry of Cyt-*c* from horse heart (solid curve a) and Cyt-c_1 (solid curve b) and Cu_A from *T. thermophilus* (solid curve c) immobilized on gold nanoparticles modified with DTSP in 50 mM KPi buffer (pH 8) (scan rate $\nu = 0.1$ V s^{-1}). The dotted curves represent the respective backgrounds.

negative staining with uranyl acetate. The background also showed some free proteins that were not totally removed during the sample preparation. As a control experiment, nonmodified nanoparticles (Figure 3a) were also negatively stained. The average diameter of 15 nm was confirmed with the measurement of around 600 particles from each set.

Electrochemical Behavior of the Immobilized Enzymes. The electrochemical behavior of the immobilized enzymes was studied by cyclic voltammetry in argon-degassed 50 mM KPi (pH 8) buffer at 25 °C (Figures 4 and 5). The measured midpoint potentials, the protein coverages (Γ), the full width at half-height of the cathodic peak at 0.1 V s^{-1} (fwhh), and the electron transfer (ET) rates are collected in Table 1. The protein coverage relative to the surface of the gold electrode before deposition of the NPs was estimated by integration of the cathodic or anodic peaks, whereas the electron transfer rates were determined using Laviron's theory[54] from the peak-to-peak separations at high scan rates (see Supporting Information S6 and S7).

These enzyme-based electrodes showed well-defined cathodic and anodic signals, and the linear dependency of the peak current on the scan rate (see Supporting Information S5) confirmed that these signals belong to redox species immobilized on the surface of the electrode. However, only weak and irreversible signals could be obtained with Cyt-c_{552} on DTSP-modified gold nanoparticles or with Cyt-c_1 on mixed thiol SAMs, which emphasizes

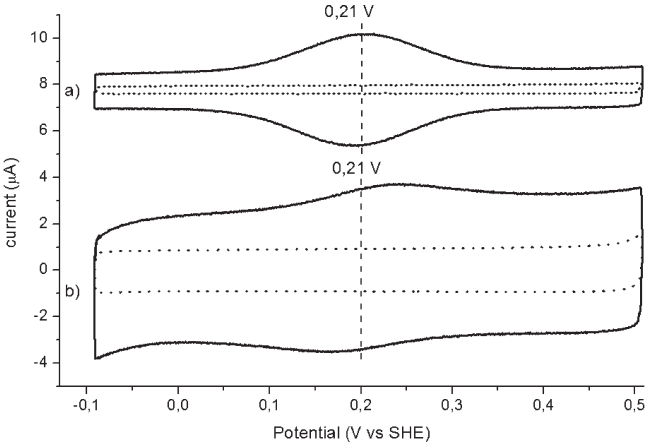

Figure 5. Cyclic voltammetry of Cu_A (solid curve a) and Cyt-c_{552} (solid curve b) from *T. thermophilus* immobilized on gold nanoparticles modified with a mixed SAM of 6-mercaptohexan-1-ol and hexanethiol in 50 mM KPi buffer (pH 8) ($\nu = 0.1$ V s^{-1}). The dotted curves represent the respective backgrounds.

again the determining role of the gold-modifier in providing a convenient support for protein immobilization and electronic coupling with the electrode. The good agreement between the midpoint potentials of the immobilized enzymes and their counterparts in solution (Table 1) suggests again that the proteins retain most of their structural integrity when immobilized. In a general way, the immobilization with DTSP leads to larger shifts of the redox potentials than the immobilization with mixed SAMs of 6-mercaptohexan-1-ol and hexanethiol. This is probably a consequence of the different interactions involved between the protein and the support, i.e., covalent in the first case and mainly hydrophobic in the second case. The largest shift (55 mV) is observed in the case of the reference protein, horse heart cytochrome *c*, and is comparable to that observed with carboxylic acid-terminated SAMs.[27] This observation is not surprising, since the covalent link probably also involves one of the surface lysine residues close to the heme cofactor in this protein. The midpoints potentials measured here for the immobilized Cyt-c_{552} and Cu_A on gold nanoparticles are also consistent with those measured on other types of electrodes (0.21 V for Cyt-c_{552} on a silver plate electrode at pH 7.6[47] and 0.22 V for Cu_A on a gold bead electrode at pH 4.6[48]). The midpoint potential of the soluble fragment of Cyt-c_1 from *T. thermophilus* compares well with that of another soluble Cyt-c_1 fragment (0.19 V vs SHE for *Paracoccus denitrificans*[55]).

The protein coverage with respect to the real surface area of the nanostructured electrode is consistent with the value for a quasi-monolayer coverage (15 pmol/cm^2) in the case of all protein and modifiers tested here. With respect to the initial surface of the gold electrode, i.e., before deposition of the nanoparticles, this is equivalent to a high number of monolayers (up to 194 in the case of Cu_A immobilized on the mixed alkyl thiol SAM; see Table 1). These results emphasize the high specific surface area of the three-dimensional gold nanoparticle electrodes and show that the method of Nakamura et al.[27] can be extended to different kinds of proteins. Only the modifier of the gold surface needs to be adapted. In the approach presented here, cytochrome *c* exchanges electrons with the electrode even faster than in the case of 11-mercaptoundecanoic acid-modified gold NPs reported (k = 13 s^{-1}),[27] which could in part be due to the

Table 1. Midpoint Potentials ($E_{1/2\,im}$), Full Width at Half-Height of the Cathodic Peak at 0.1 V s^{-1} (fwhh), Surface Coverages (Γ) with Respect to the Initial Surface Area of the Gold Electrode, ET Rates of the Immobilized Cyt-*c*, Cyt-c_1, Cu_A, and Cyt-c_{552}, and Comparison with the Midpoint Potentials in Solution ($E_{1/2\,sol}$)

enzyme	$E_{1/2\,sol}$ (V)	$E_{1/2\,im}$ (V)	fwhh (mV)	Γ (pmol/cm^2)	ET rate (s^{-1})
Cyt-*c* (DTSP)	0.27[58]	0.22	102	1700	30
Cyt-c_1 (DTSP)	0.14[a]	0.16	101	2000	23
Cu_A (DTSP)	0.24[59]	0.20	112	2900	3
Cu_A (mixed SAM)	0.24[59]	0.21	140	2100	31
Cyt-c_{552} (mixed SAM)	0.20[60]	0.21	135	1000	18

[a] Value obtained by a potentiometric UV/visible titration (data not shown).

shorter length of the modifier in our case. The other enzymes of this study showed generally good electron transfer rates with the electrode, promoted by the gold nanoparticles as well. The case of Cu_A is particularly interesting. It is clear than the electron transfer efficiency is better when immobilization is performed on gold nanoparticles modified with mixed SAMs of alkyl thiol and hydroxyl-terminated alkyl thiol than with DTSP. This coupling agent requires some primary amines to react, such as that of lysine side chains, but no such polar residue can be found in the highly hydrophobic region close to the copper center, where the redox partner of the protein is believed to bind.[37,48] The closest lysines are located 20 Å away from the cofactor (see Supporting Information S8). The arginines 59 and 146 located 11−13 Å away might be alternative positions of attachment. Therefore, DTSP-modified nanoparticles will not be as close to the cofactor as alkyl thiol-modified gold surfaces, which are suited to bind in the hydrophobic region close to the copper center.[48] Similarly, the heme edge of Cyt-c_{552} is largely uncharged,[46] which prevents attachment of the modifier close to the cofactor and therefore explains why only weak electrochemical signals were observed for Cyt-c_{552} immobilized on DTSP-modified gold nanoparticles. In contrast, the good electron transfer rate obtained for Cyt-c_1 using this modification strongly suggests the attachment through lysines close to the heme cofactor.

For redox species homogeneously immobilized on the surface of electrodes and involved in reversible electrochemical processes, the fwhh of the signals should be 90.6 mV.[56] The observed values are close to the ideal value in the case of Cyt-*c* and Cyt-c_1 immobilized on DTSP-modified gold nanoparticles, confirming the good electronic communication between the enzymes and the electrode. However, the values are significantly larger for enzymes immobilized on mixed-SAM-modified gold nanoparticles. Studies with cytochrome *c* immobilized on gold electrodes modified with carboxylic acid-terminated alkylthiols have suggested that such a nonideal behavior is linked to a distribution of interfacial microenvironments for the adsorbed proteins.[57] It is reasonable to propose that when a mixture of thiols is used, a larger variety of adsorption sites for the protein exist on the gold surface, leading to a larger distribution of formal potentials.

4. CONCLUSION

We have successfully immobilized two soluble heme proteins and one copper protein derived from the respiratory chain of *T. thermophilus*, Cyt-c_1, Cyt-c_{552}, and Cu_A, on gold nanoparticles deposited on the surface of a polycrystalline gold electrode. We have considered different modifications of the gold nanoparticles, DTSP and alkyl thiols. A satisfying electron transfer was established between the immobilized enzymes and the electrode, and midpoint potentials were comparable to those measured in solution. SEIRAS studies confirmed the successful immobilization as well as the integrity of the immobilized proteins. Three-dimensional gold nanoparticle electrodes can therefore be used as an efficient support of immobilization of several different kinds of proteins. These studies also open the way to the immobilization of the larger respiratory membrane proteins of *T. thermophilus* and related systems.

■ ASSOCIATED CONTENT

Supporting Information. UV/vis spectrum of the gold nanoparticles, voltammogram of the gold electrode before and after deposition of the gold NPs, amide I and amide II regions of the SEIRAS spectra of the immobilized enzymes, cathodic current versus scan rate plots, trumpet and Laviron plots of the immobilized enzymes, and a cartoon view of the Cu_A protein. This material is available free of charge via the Internet at http://pubs.acs.org.

■ AUTHOR INFORMATION

Corresponding Author
*E-mail: hellwig@unistra.fr (P.H.); fmelin@unistra.fr (F.M.).

■ ACKNOWLEDGMENT

This work was supported by CNRS (Centre National de la Recherche Scientifique), ANR (Agence National de Recherche), and the "Conseil Scientifique" of the University of Strasbourg. The authors are indebted to Prof. Dr. James A. Fee and Dr. Ying Chen (the Scribbs Research Institute, La Jolla, California) for a generous gift of the Cu_A protein.

■ REFERENCES

(1) Wang, J. *Chem. Rev.* **2007**, *108*, 814–825.
(2) Heller, A. *Phys. Chem. Chem. Phys.* **2004**, *6*, 209–216.
(3) Kim, J.; Jia, H.; Wang, P. *Biotechnol. Adv.* **2006**, *24*, 296–308.
(4) Minteer, S. D.; Liaw, B. Y.; Cooney, M. J. *Curr. Opin. Biotechnol.* **2007**, *18*, 228–234.
(5) Neto, S.; Forti, J.; De Andrade, A. *Electrocatal.* **2010**, *1*, 87–94.
(6) Murgida, D. H.; Hildebrandt, P. *Phys. Chem. Chem. Phys.* **2005**, *7*, 3773–3784.
(7) Hirst, J. *Biochim. Biophys. Acta, Bioenerg.* **2006**, *1757*, 225–239.
(8) Reda, T.; Hirst, J. *J. Phys. Chem. B* **2006**, *110*, 1394–1404.
(9) Willner, I.; Katz, E. *Angew. Chem., Int. Ed.* **2000**, *39*, 1180–1218.
(10) Moehlenbrock, M. J.; Minteer, S. D. *Chem. Soc. Rev.* **2008**, *37*, 1188–1196.
(11) Akers, N. L.; Moore, C. M.; Minteer, S. D. *Electrochim. Acta* **2005**, *50*, 2521–2525.
(12) Lim, J.; Malati, P.; Bonet, F.; Dunn, B. *J. Electrochem. Soc.* **2007**, *154*, A140–A145.
(13) Katz, E.; Sheeney-Haj-Ichia, L.; Willner, I. *Angew. Chem., Int. Ed.* **2004**, *43*, 3292–3300.
(14) Cabrita, J. F.; Abrantes, L. M.; Viana, A. S. *Electrochim. Acta* **2005**, *50*, 2117–2124.
(15) Beneyton, T.; El Harrak, A.; Griffiths, A. D.; Hellwig, P.; Taly, V. *Electrochem. Commun.* **2011**, *13*, 24–27.

(16) Xiao, Y.; Patolsky, F.; Katz, E.; Hainfeld, J. F.; Willner, I. *Science* **2003**, *299*, 1877–1881.
(17) Pingarrón, J. M.; Yáñez-Sedeño, P.; González-Cortés, A. *Electrochim. Acta* **2008**, *53*, 5848–5866.
(18) Kim, J.; Grate, J. W.; Wang, P. *Trends Biotechnol.* **2008**, *26*, 639–646.
(19) Willner, I. *FEBS J.* **2007**, *274*, 301–301.
(20) Yan, Y.-M.; Tel-Vered, R.; Yehezkeli, O.; Cheglakov, Z.; Willner, I. *Adv. Mater.* **2008**, *20*, 2365–2370.
(21) Yan, Y.-M.; Baravik, I.; Tel-Vered, R.; Willner, I. *Adv. Mater.* **2009**, *21*, 4275–4279.
(22) Yehezkeli, O.; Raichlin, S.; Tel-Vered, R.; Kesselman, E.; Danino, D.; Willner, I. *J. Phys. Chem. Lett.* **2010**, *1*, 2816–2819.
(23) Abad, J. M.; Gass, M.; Bleloch, A.; Schiffrin, D. J. *J. Am. Chem. Soc.* **2009**, *131*, 10229–10236.
(24) Rahman, M. A.; Noh, H.-B.; Shim, Y.-B. *Anal. Chem.* **2008**, *80*, 8020–8027.
(25) Feng, J.-J.; Zhao, G.; Xu, J.-J.; Chen, H.-Y. *Anal. Biochem.* **2005**, *342*, 280–286.
(26) Jensen, P. S.; Chi, Q.; Grumsen, F. B.; Abad, J. M.; Horsewell, A.; Schiffrin, D. J.; Ulstrup, J. *J. Phys. Chem. C* **2007**, *111*, 6124–6132.
(27) Murata, K.; Kajiya, K.; Nukaga, M.; Suga, Y.; Watanabe, T.; Nakamura, N.; Ohno, H. *Electroanalysis* **2010**, *22*, 185–190.
(28) Aubin-Tam, M.-E.; Hamad-Schifferli, K. *Langmuir* **2005**, *21*, 12080–12084.
(29) Hung, A.; Mwenifumbo, S.; Mager, M.; Kuna, J. J.; Stellacci, F.; Yarovsky, I.; Stevens, M. M. *J. Am. Chem. Soc.* **2011**, *133*, 1438–1450.
(30) Mooser, D.; Maneg, O.; Corvey, C.; Steiner, T.; Malatesta, F.; Karas, M.; Soulimane, T.; Ludwig, B. *Biochim. Biophys. Acta, Bioenerg.* **2005**, *1708*, 262–274.
(31) Than, M. E.; Hof, P.; Huber, R.; Bourenkov, G. P.; Bartunik, H. D.; Buse, G.; Soulimane, T. *J. Mol. Biol.* **1997**, *271*, 629–644.
(32) Williams, P. A.; Blackburn, N. J.; Sanders, D.; Bellamy, H.; Stura, E. A.; Fee, J. A.; McRee, D. E. *Nat. Struct. Mol. Biol.* **1999**, *6*, 509–516.
(33) Slutter, C. E.; Sanders, D.; Wittung, P.; Malmstrom, B. G.; Aasa, R.; Richards, J. H.; Gray, H. B.; Fee, J. A. *Biochemistry* **1996**, *35*, 3387–3395.
(34) Mooser, D.; Maneg, O.; MacMillan, F.; Malatesta, F.; Soulimane, T.; Ludwig, B. *Biochim. Biophys. Acta, Bioenerg.* **2006**, *1757*, 1084–1095.
(35) Janzon, J.; Ludwig, B.; Malatesta, F. *IUBMB Life* **2007**, *59*, 563–569.
(36) Maneg, O.; Malatesta, F.; Ludwig, B.; Drosou, V. *Biochim. Biophys. Acta, Bioenerg.* **2004**, *1655*, 274–281.
(37) Soulimane, T.; Buse, G.; Bourenkov, G. P.; Bartunik, H. D.; Huber, R.; Than, M. E. *EMBO J.* **2000**, *19*, 1766–1776.
(38) Maneg, O.; Ludwig, B.; Malatesta, F. *J. Biol. Chem.* **2003**, *278*, 46734–46740.
(39) Turkevich, J.; Stevenson, P. C.; Hillier, J. *Discuss. Faraday Soc.* **1951**, 55–75.
(40) Frens, G. *Nat. Phys. Sci.* **1973**, *241*, 20–22.
(41) Trasatti, S.; Petrii, O. A. *Pure Appl. Chem.* **1991**, *63*, 711–734.
(42) Haiss, W.; Thanh, N. T. K.; Aveyard, J.; Fernig, D. G. *Anal. Chem.* **2007**, *79*, 4215–4221.
(43) Arya, S. K.; Pandey, P.; Singh, S. P.; Datta, M.; Malhotra, B. D. *Analyst* **2007**, *132*, 1005–1009.
(44) Chen, X. J.; West, A. C.; Cropek, D. M.; Banta, S. *Anal. Chem.* **2008**, *80*, 9622–9629.
(45) Bernad, S.; Soulimane, T.; Lecomte, S. *J. Raman Spectrosc.* **2004**, *35*, 47–54.
(46) Bernad, S.; Soulimane, T.; Mehkalif, Z.; Lecomte, S. *Biopolymers* **2006**, *81*, 407–418.
(47) Bernad, S.; Leygue, N.; Korri-Youssoufi, H.; Lecomte, S. *Eur. Biophys. J.* **2007**, *36*, 1039–1048.
(48) Fujita, K.; Nakamura, N.; Ohno, H.; Leigh, B. S.; Niki, K.; Gray, H. B.; Richards, J. H. *J. Am. Chem. Soc.* **2004**, *126*, 13954–13961.
(49) Ataka, K.; Giess, F.; Knoll, W.; Naumann, R.; Haber-Pohlmeier, S.; Richter, B. r.; Heberle, J. *J. Am. Chem. Soc.* **2004**, *126*, 16199–16206.
(50) Ataka, K.; Heberle, J. *Anal. Bioanal. Chem.* **2007**, *388*, 47–54.
(51) Ojea-Jimenez, I.; Romero, F. M.; Bastus, N. G.; Puntes, V. *J. Phys. Chem. C* **2010**, *114*, 1800–1804.
(52) Barth, A. *Biochim. Biophys. Acta, Bioenerg.* **2007**, *1767*, 1073–1101.
(53) Oberg, K. A.; Ruysschaert, J.-M.; Goormaghtigh, E. *Eur. J. Biochem.* **2004**, *271*, 2937–2948.
(54) Laviron, E. *J. Electroanal. Chem.* **1979**, *101*, 19–28.
(55) Janzon, J.; Yuan, Q.; Malatesta, F.; Hellwig, P.; Ludwig, B.; Durham, B.; Millett, F. *Biochemistry* **2008**, *47*, 12974–12984.
(56) *Electrochemical Methods: Fundamentals and Applications*, 2nd ed.; Bard, A. J., Faulkner, L. R., Eds.; Wiley: New York, 2001.
(57) Clark, R. A.; Bowden, E. F. *Langmuir* **1997**, *13*, 559–565.
(58) Gopal, D.; Wilson, G. S.; Earl, R. A.; Cusanovich, M. A. *J. Biol. Chem.* **1988**, *263*, 11652–11656.
(59) Immoos, C.; Hill, M. G.; Sanders, D.; Fee, J. A.; Slutter, C. E.; Richards, J. H.; Gray, H. B. *J. Biol. Inorg. Chem.* **1996**, *1*, 529–531.
(60) Fee, J. A.; Chen, Y.; Todaro, T. R.; Bren, K. L.; Patel, K. M.; Hill, M. G.; Gomez-Moran, E.; Loehr, T. M.; Ai, J.; Thöny-meyer, L.; Williams, P. A.; Sturam, E.; Sridhar, V.; McRee, D. E. *Protein Sci.* **2000**, *9*, 2074–2084.